

EXPERIMENTAL DETERMINATION OF DYNAMIC CHARACTERISTICS OF THE IMPELLER-BEARING-HOUSING SYSTEM OF VENTRASSIST™ BLOOD PUMP

N. Zhang¹, M. Chung¹ and G.D. Tansley²

¹ Faculty of Engineering, University of Technology, Sydney, 1 Broadway NSW 2007, Australia

² School of Mechanical, Materials, Manufacturing, Engineering and Management, The University of Nottingham, University Park, Nottingham NG7 2RD, United Kingdom

ABSTRACT

This paper presents an experimental investigation of the dynamic coefficients of the hydrodynamic bearing of the rotary blood pump for various pump speeds. A special test rig was developed to enable the measurements of pump housing absolute displacement and the impeller displacements relative to the housing to be taken simultaneously during the operation of the pump. From the measured decaying sine wave displacement, the natural frequency, damping and stiffness coefficients of the impeller-bearing-housing system were determined. Results indicate that stiffness and damping coefficients increased as flow rate and pump speed increased, representing an increase in stability with these changing conditions.

1. INTRODUCTION

The VentrAssist™ implantable rotary blood pump is based on a centrifugal design and is intended for long term ventricular assist. It is a novel device consisting of only one moving part – a shaftless impeller. The impeller blades are imbedded with permanent magnets to enable the impeller to act as a rotor for the pump's brushless DC motor. Due to the absence of a shaft, contact bearings and seals, the design of the pump is ideal for reducing blood trauma that may lead to haemolysis and thrombosis. This is because the rubbing at contact points between a shaft and bearings can cause damage to red blood cells through shearing and heat. Blood clots or thrombosis can also be experienced due to stagnant flow at these contact points and at the seals. Suspension of the impeller in radial and axial directions within the blood pump cavity is achieved purely through the use of hydrodynamic bearings. Hydrodynamic suspension systems have been investigated by other parties [1-4]. However these systems work in synergy with magnetic bearings for actively controlled suspension combining magnetic thrust bearings with hydrodynamic bearings to achieve full support of the rotor. Total active suspension systems through magnetic bearings are currently being utilised by other rotary blood pumps [5-7] that use complex and large monitoring and electrical systems. Besides the VentrAssist™ rotary blood pump, there are currently no rotary blood pumps which rely purely on hydrodynamic wedge bearings. With the VentrAssist™ pump, monitoring sensors are eliminated due to the use of hydrodynamic bearings for passive suspension and thus less complicated electronics are required. It results in a smaller, more efficient and reliable pump requiring fewer electrically dependent components.

Through the implementation of a hydrodynamic bearing for passive suspension of the impeller, the dynamic characteristics of the system were unique and the analysis was challenging. This paper presents an experimental investigation of the dynamic coefficients of the hydrodynamic bearing of the rotary blood pump for various pump speeds. The dynamic coefficients are represented by linearised stiffness and damping coefficients of the hydraulic bearing that is formed by the impeller, fluids (blood) and pump housing. A special test rig was developed to enable the measurements of pump housing absolute displacement and the impeller displacements relative to the housing to be

taken simultaneously during the operation of the pump. The displacement measurements were taken when an impulsive disturbance force was exerted onto the pump housing that caused the impeller to be displaced from its dynamic equilibrium within the pump cavity. The Hall Effect sensors, developed for obtaining displacement measurements accurately [8], were used for the experimental investigation. From the decaying sine wave, the natural frequency, damping and stiffness coefficients of the impeller-bearing-housing system were determined. The results and discussions are presented.

2. MATERIALS AND EXPERIMENTAL SETUP

A laboratory version of a VentrAssist™ C-D pump housing and a 2.8 series impeller (Fig. 1) was used for the experiment, where the impeller had a mass of 35 g (0.035 kg), with outside diameter of 40 mm and the cone angle of 45°. The pump housing and impeller were made of titanium-aluminium-vanadium (Ti-6Al-4V), a biocompatible alloy.

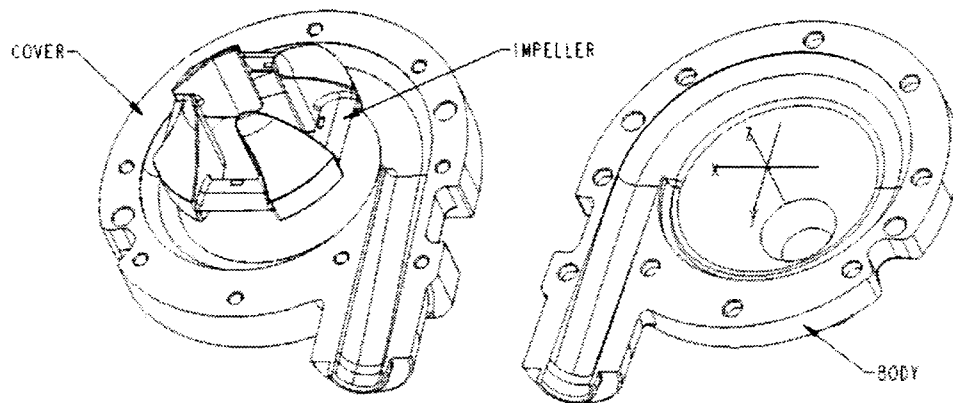


Figure 1: Titanium C-D pump housing and 2.8 impeller

Four Hall Effect sensors (91SS12-2 – Honeywell, U.S.A.) were placed on the bottom of the cover in x-y plane. The location and setup of the sensors was identical to previous investigations [8]. The measurements from the sensors were amplified through custom designed operational amplifiers. Amplified signals were sent to an analogue breakout accessory rack and data acquisition board where the signals were data logged and displayed. The details of the instrumentation can be found in reference [8]. All sensors were calibrated individually for each pump speed to ensure the accurate transformation of the output voltage into displacement (μm) values. Calibration polynomials were determined through the least squares method. Orders of polynomials were determined by residual plots as well as calculation of variances.

Eight pump operating conditions were investigated. The speed of the pump was adjusted through the motor controller, while the outflow of the pump was partially throttled to achieve the flow rates required for each condition. The flow rate was monitored by a flow probe and a flow meter. These operating conditions were flow rate of 3, 4 and 5 L/min at speeds of 2000, 2300 and 2500 RPM. Data at 3 L/min and 2500 rev/min is not presented since the old version of the controller used was not able to hold the set speed sufficiently accurately.

The pumping medium used for the experiment was 30% aqueous glycerol. Properties of 30% aqueous glycerol with 0.9% sodium chloride solution and blood are shown in Table 1.

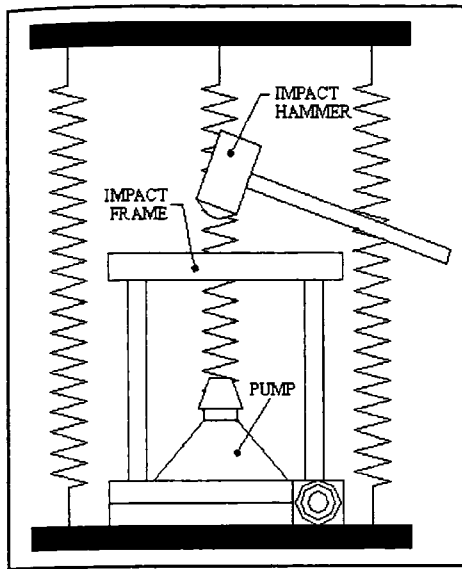


Figure 2: Pump on a suspension system

The pump was mounted on a suspension system consisting of a platform suspended with springs as shown in Figure 2. The top boundary of the platform was fixed to the ground. The platform with the mounted pump and impact frame had a total mass of 0.65 kg. The suspension system was designed to ensure that its natural frequency and damping ratio did not coincide with the natural frequency and damping ratio of the impeller-hydrodynamic bearing-housing system. To determine the natural frequency and damping ratio of the suspension system, the platform together with the complete pump setup was given a vertical impulsive disturbance. The response of the system to this disturbance was measured using a piezo-electric accelerometer producing a sine wave that decayed over time. From this decaying sine wave, the natural frequency and damping ratio of the suspension system was calculated using logarithmic decrement methods. More detailed information on the instrumentation and similar entire experimental setup of the pump can be found in reference [8].

For each pump operating condition, a vertical impulsive force was applied to the pump via the impact frame mounted on top of the pump, to disturb the impeller from its equilibrium (axially). The magnitude of the impulse force required to disturb the impeller was within a range that did not cause large impeller motion. As the logarithmic decrement method was based on the ratio between the amplitudes of two sequential response cycles and the response period, for different magnitudes of impulsive force, identical damping ratio and damped natural frequency can be determined. The disturbance from the impact caused the hydrodynamic bearing to dynamically stabilise the impeller back to its equilibrium. After disturbance, the axial displacement of the impeller for every blade passing each sensor for a time period of one second was measured. These measurements produced a free decaying curve, which allowed for the logarithmic decrement method to be applied and dynamic characteristics calculated at each sensor location on the bearing pad. All measurements were acquired at a sampling frequency of 20 kHz. A bandpass filter was implemented to allow for increased signal-to-noise ratio and in a particular frequency range. To determine an ideal frequency range for the bandpass filter, the filter was initially set at a frequency range of 10 – 250 Hz and FFT analysis was performed. The analysis showed a dominant peak between the frequencies of 10 Hz and 20 Hz, indicating a possible natural frequency presence in this range. Therefore, for final measurements the bandpass filter was set within the frequency range of 10 Hz – 20 Hz.

Figure 3 shows a linearised hydraulic bearing model represented by a linear spring and damper. The stiffness and damping coefficients of the hydrodynamic bearing were determined from measured

Table 1: Fluids contents used for pump test

Property	Aqueous Glycerol	40% Hematocrit Blood
Viscosity (mPas)	3.3	4.3
Density (kg/m ³)	1.0786	1.055

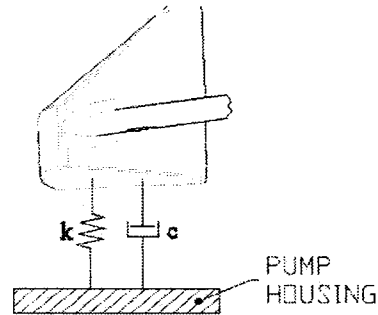


Figure 3: Linearised hydraulic bearing model

free decay response of the impellor relative to pump housing under an impulse input. The average of these stiffness and damping coefficients obtained from a few measurements taken under same operational conditions and test setting are computed to minimise the errors in measurements and environmental noise influence.

3. RESULTS

The total mass of the blood pump and the platform was 0.65 kg. The natural frequency of the suspension system of the test rig was experimentally determined as 4 Hertz that is well away from the natural frequency of the impellor-bearing-housing system. The damping ratio of the suspension system was identified as 0.0365.

The low natural frequency and damping ratio of the test platform suspension system allowed its dynamic characteristics to be isolated from the dynamic characteristics of the impeller-bearing-housing system. Therefore, the band-pass filter for bearing system measurements was set at a high pass frequency of 10 Hz and a low pass frequency of 20 Hz. This frequency range was less than the pump speed frequency of 33.33Hz, 38.33Hz and 41.67Hz for pump speeds of 2000, 2300 and 2500 rev/min respectively and greater than the natural frequency of 4 Hz of the suspension system.

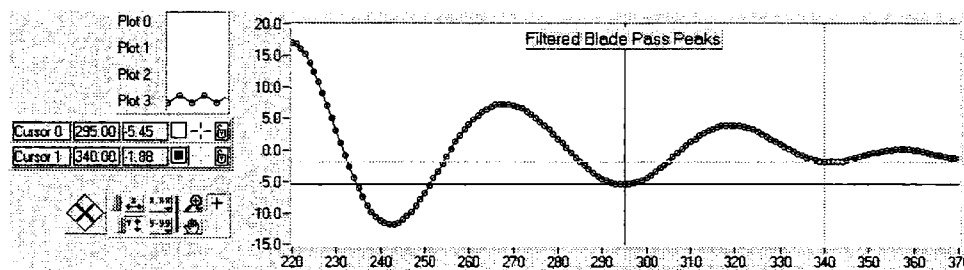


Figure 4: Example of free decaying curve used for logarithmic decrement calculations

Figure 4 shows an example of a free decaying curve that was plotted from one of the measurements. This example was an actual free decay response that was measured and used to determine the dynamic characteristic of the system for a pump speed of 2300 rev/min and a flow rate of 5 L/min and shows the high clarity of signal post filtering. In the figure, the vertical axis represents the measured displacement of the impeller relative to the pump housing and the unit is in μm . The horizontal axis represents the numbering of the data that can be converted to time as the sampling frequency is known.

The period of the response is determined from the plot and then the damped angular frequency is calculated. The logarithmic decrement is determined from two measured amplitudes of the two neighbouring cycles of responses and then the damping ratio is then calculated. Consequently, the stiffness and damping coefficients of the system are determined as the impeller mass is pre-known.

The above signal process was repeated to determine the dynamic characteristics of the impeller-hydrodynamic bearing-housing system for different flow rates and three pump speeds. The obtained results are presented in Table 2.

Table 2: Dynamic characteristics of the impeller-hydrodynamic bearing-housing system at sensor locations for changing flow rates at pump speeds of 2000, 2300 and 2500 rev/min.

Pump Speed (rev/min)	Flow Rate (L/min)	Mean Natural Frequency (Hz)	Mean Damping Ratio	Total Stiffness Coefficient (N/m)	Total Damping Coefficient (N.s/m)
2000	3	12.60	0.14	877.39	3.08
	4	13.49	0.15	1005.94	3.62
	5	13.85	0.16	1060.47	3.88
2300	3	12.92	0.15	922.53	3.31
	4	13.22	0.16	965.28	3.67
	5	13.82	0.16	1055.37	4.00
2500	4	14.27	0.18	1125.55	4.52
	5	14.84	0.19	1217.88	4.96

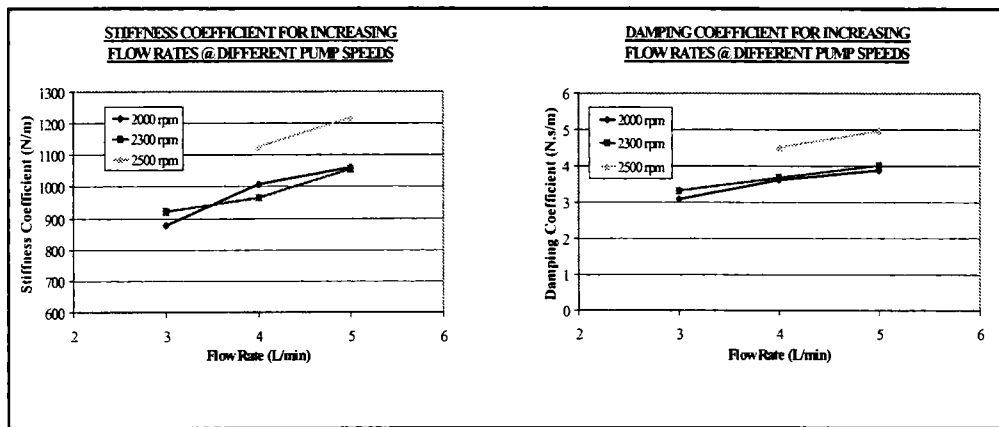


Figure 5: Stiffness coefficient (left) and damping coefficient (right) of the hydrodynamic bearing with respect to different flow rates and pump speeds

Figure 5 shows the plots of the obtained stiffness and damping coefficients of the impeller-bearing-pump housing system. The plots show that the stiffness and damping coefficients become larger when the pump flow rate increases. There is insignificant difference between the dynamic characteristics obtained at the pump speed of 2000 RPM and that obtained at 2300 RPM. However, the dynamic characteristics obtained at the pump speed of 2500 RPM are significantly different from those obtained at the other two speeds. No measurements obtained when the flow rate is 3 L/min and the pump speed is 2500 RPM as this case is out of the pump operation range.

4. DISCUSSION

For centrifugal pumps, the flow rate is influenced by the angular speed of the impeller and head rise across the pump with fixed pump configuration. The displacement of the impeller has insignificant influence on the flow rate and this has been confirmed from previous investigations [8]. From Figure 5 it is seen that the stiffness and damping coefficients of the system increased linearly with respect to flow rates. However, the increases of these coefficients for fixed for rates were more dramatic for a speed change from 2300 rev/min to 2500 rev/min than a change from 2000 rev/min to 2300 rev/min. This indicated that both the stiffness and damping coefficients of the impeller-bearing-housing system increased significantly for pump speeds between 2300 and 2500 RPM, thus

made it harder for the impeller to move away from its equilibrium under disturbances.

The theoretical analysis of the relationship between the dynamic characteristics of the hydraulic bearing, the tangential fluid velocity and the flow rate suggests that as velocity increased, the dynamic coefficients of the system increased as its squared function. And the dynamic coefficients, increase linearly with respect to the flow rate increase. Hence, the velocity has a greater influence on the dynamic coefficients of the impeller-bearing-housing system than the pump flow rate.

Since the square of natural frequency of the impeller-bearing-housing system is proportional to the stiffness coefficient, it becomes higher when the flow rate increases and/or the pump speed increases. This is demonstrated from the obtained results given in Table 2. The obtained damping ratio of the system, shown the Table 2, also increases significantly when the flow rate and/or the pump speed increases. The significant increase of the damping coefficient means that the impeller would be stabilised quickly and efficiently under disturbances.

5. CONCLUSIONS

The dynamic characteristics of the impeller-hydrodynamic bearing-housing were determined experimentally under three pump speeds and three flow rates. A vertical external impulse force was applied to the pump housing mounted on a specially designed test platform, which caused the impeller to be displaced from its dynamic equilibrium. The Hall Effect sensors were developed to measure the displacement of the impeller. Values for natural frequency, damping ratio, stiffness coefficient and damping coefficient were identified from the measurements of displacement of the impeller relative to the pump housing. These values increased as flow rate and pump speed increased, indicating that the dynamic stability of the bearing increased with the changing conditions. However, pump speed had a greater influence on the values than flow rate, which was evident through dynamic analysis. It is fair to conclude that the impeller-bearing-housing system is dynamically stable within the specified operational range.

ACKNOWLEDGEMENTS

Financial support for this research was provided jointly by the Australian Research Council (Grant No. C89920011), the University of Technology, Sydney and Ventracor Limited Australia.

REFERENCES

- [1] Kung RT, Hart RM. Design considerations for bearingless rotary pumps. *Artificial Organs* 1997, Vol. 21, pp. 645-50.
- [2] Malanoski SB, Belawski H, Horvath D, Smith WA, Golding LR. Stable blood lubricated hydrodynamic journal bearing with magnetic loading. *ASAIO Journal* 1998, 44:M737-40.
- [3] Wampler R, Lancisi D, Indravudh V, Gauthier R, Fine R. A sealless centrifugal blood pump with passive magnetic and hydrodynamic bearings. *Artificial Organs* 1999 Vol 23, pp.780-4.
- [4] Xu L, Wang F, Fu M, Medvedev A, Smith WA, Golding LR. Analysis of a new PM motor design for a rotary dynamic blood pump. *ASAIO Journal* 1997, 3:M559-64.
- [5] Masuzawa T, Kita T, Matsuda K, Okada Y. Magnetically Suspended Rotary Blood pump with radial type combined motor-bearing. *Artificial Organs* 2000, Vol. 24, pp. 468-74.
- [6] Allaire P, Hilton E, Baloh M, Maslen E, Bearson G, Noh D, Khanwilkar P, Olsen D. Performance of a continuous flow ventricular assist device: Magnetic bearing design, construction, and testing. *Artificial Organs* 1998, Vol. 22, pp.475-80.
- [7] Akamatsu T, Nakazeki T, Itoh H. Centrifugal blood pump with a magnetically suspended impeller. *Artificial Organs* 1992 Vol. 16, pp. 305-8.
- [8] Chung M, Zhang N, Tansley GD, Woodard JC. Impeller behaviour and displacement of the VentrAssist implantable rotary blood pump. *Artificial Organs* 2004 Vol.28, pp. 287-297.